ASSOCIAZIONE NAZIONALE ITALIANA DI INGEGNERIA SISMICA
ANIDIS
Italian National Association of Earthquake Engineering

XVIII CONVEGNO ANIDIS
L'ingegneria sismica in Italia
ASCOLI PICENO 2019
15-19 Settembre

Pushover analysis of reinforced concrete framed structures: comparison between response obtained using beam or multi-layered shell elements

Beatrice Belletti[a], Simone Ravasini[a], Francesca Vecchi[a]
[a] *Dipartimento di Ingegneria e Architettura, Parco Area delle Scienze, 181A Parma, Italy*

Keywords: seismic vulnerability, reinforced concrete, PARC_CL 2.0, plastic deformations

ABSTRACT
In the context of the seismic vulnerability assessment of existing reinforced concrete buildings, the load-carrying capacity of structures is strongly affected by steel and concrete mechanical properties and construction details. In this work, the institute "A. De Gasperi – R. Battaglia", located in Norcia, has been chosen as case study. Two different modelling strategies have been adopted by using beam elements or multi-layered shell elements for the structural schematization. The non-linear behavior of shell elements is evaluated using the PARC_CL 2.0 crack model, implemented in Abaqus Code as user subroutine. The non-linear ductile behavior of beam elements is evaluated using, at each integration point, the moment/curvature and the axial force/strain relationships which are uncoupled. Brittle failure mode in columns, beams and beam-to-column joints are calculated from the demand via post-processing of the results obtained from beam modelling and the capacity from analytical formulations provided by Italian NCT 2018 and Eurocode 8 Standard Code. The main scope of this paper is thus the evaluation of the structural response and damage grade detection of the case study by using nonlinear finite element analyses, highlighting the benefits of using beam or shell element modeling.

1 INTRODUCTION

The performances of existing structures subjected to seismic actions are strongly affected by material properties and construction details. In particular, the majority of existing reinforced concrete structures have been designed to sustain only the gravitational loads, without paying attention to the seismic performances. For this reason, the capacity assessment of the structure in terms of ductile and brittle failure modes of seismic resisting members becomes critical under seismic conditions. The seismic response of a building is characterized by different damage grades corresponding to different base accelerations, as described in EMC 98 document (Grunthal, 1998). Detailed finite element models (for example shell element modelling) could be able to detect the different damage grades during the structural response, conversely simplified models (for example beam elements modelling), coupled with conservative analytical formulations, could lead to damage assessments which are different from the realistic behaviour of the structure. Therefore, nonlinear finite element analyses are a fundamental tool in order to investigate the mentioned phenomena, which could lead to different design strategies and local interventions to prevent the collapse or to improve the behaviour of the existing structures. In this work, the ductile and brittle failures are investigated for beams, columns and joints by performing pushover analyses. For this purpose, the institute "A. De Gasperi – R. Battaglia" located in Norcia (described in detail in Lima et al. 2018) is chosen as case study, where two different types of modelling techniques are used to model the structure in Abaqus (Abaqus, 2018):

- The structure is modelled using beam elements where the mechanical behaviour of beams and columns is assigned by using nonlinear relationships for bending moment and axial force and the brittle failures are investigated by a post-processing analysis based on the formulations provided in Eurocode 8 (Eurocode 8, 2005) and NTC 2018 (NTC, 2018).

– The structure is modelled using multi-layered shell elements, where the mechanical behaviour is evaluated using the PARC_CL 2.0 crack model, implemented in Abaqus Code as user subroutine (Belletti et al., 2017a).

Finally, the evaluation of the structural response and damage grade detection is carried out by the comparison of the two different modelling techniques.

2 NUMERICAL MODELLING

2.1 Description of the structure

The existing building is characterized by a reinforced concrete framed resisting system, see Figure 1a. The floor to floor height is 3.7 m at the first floor, 3.3 m for remaining floors and 2.5 m at the roof, see Figure 1b. The columns (named from 1 to 21) present variable cross section along the height of the building with major local axis oriented along the Y direction. The beams are oriented in X direction (named for example from A12 to A67 for the bottom side of the building scheme etc.) and Y directions (named for example 7a and 7b for the right side of the building scheme etc.).

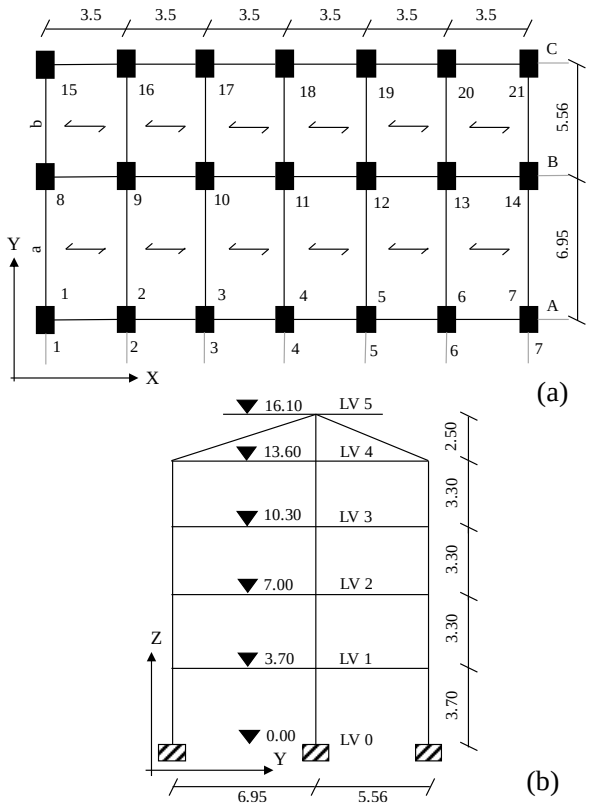

Figure 1. Building geometry: (a) plan view; (b) elevation view. Dimensions in meters.

The diaphragms at each floor are characterised by composite joists oriented along the X direction.

In this work, for both models (beam elements and multi-layered shell elements) the software Abaqus is used (Abaqus, 2018).

Pushover analyses are performed applying a mass proportional acceleration along the Y direction at each floor.

2.2 Mechanical properties, loads and mass distribution

The mechanical properties for steel and concrete are provided by in-situ tests. The mean values are reported are reported in Table 1.

Table 1. Mechanical properties of materials.

concrete			steel		
f_{cm} [MPa]	f_{ct} [MPa]	E_c [MPa]	f_{ym} [MPa]	f_u [MPa]	E_s [MPa]
25.2	2	22000	375	450	200000

Uniformly distributed loads equivalent to the contemporary static combination (self-weights, permanent and variable floor loads) are applied to beams.

For each floor level, the lumped seismic masses are distributed in correspondence of beam-to-column joints. The total seismic masses at each floor level are reported in Table 2.

Table 2 Seismic masses at each floor level and total mass.

LV 1 [tonn]	*LV 2* [tonn]	*LV 3* [tonn]	*LV 4* [tonn]	*LV 5* [tonn]	*Total* [tonn]
320	317	326	299	116	1378

2.3 Beam element modelling

For the beam element model, beams are modelled with B31 elements along the Y direction and B32 elements along the X direction. This choice has been made to reach an adequate plastic hinge length, indeed the B31 element presents two nodes and one Gauss integration point, while the B32 element presents three nodes and two Gauss integration points. The columns are modelled by using B32 elements with a length approximatively equal to the cross sectional height of the elements to provide the correct plastic hinge length. The diaphragms are modelled using truss T3D2 elements.

The compressive strength of concrete is modelled by using a parabolic behaviour until reaching a peak strain equal to 2 ‰, and considering a ultimate strain equal to 3.5 ‰. The reinforcing steel is modelled using a bilateral curve considering hardening. A steel rupture strain

ε_{rup} equal to 4 % is assumed in order to implicitly take into account premature bucking phenomena.

The mechanical nonlinearity of columns is assigned by the moment – curvature relationship at each integration point, without considering the confinement effect provided by stirrups. The moment – curvature relationship is assigned for each principal axis (1, 2) of the cross section. An additional nonlinearity due to axial behaviour is considered by assigning an axial force vs strain relationship, which results uncoupled with respect to the flexural behaviour. For example, the bending moment –curvature relationships for the columns of level LV0-LV1 are shown in Figure 2.

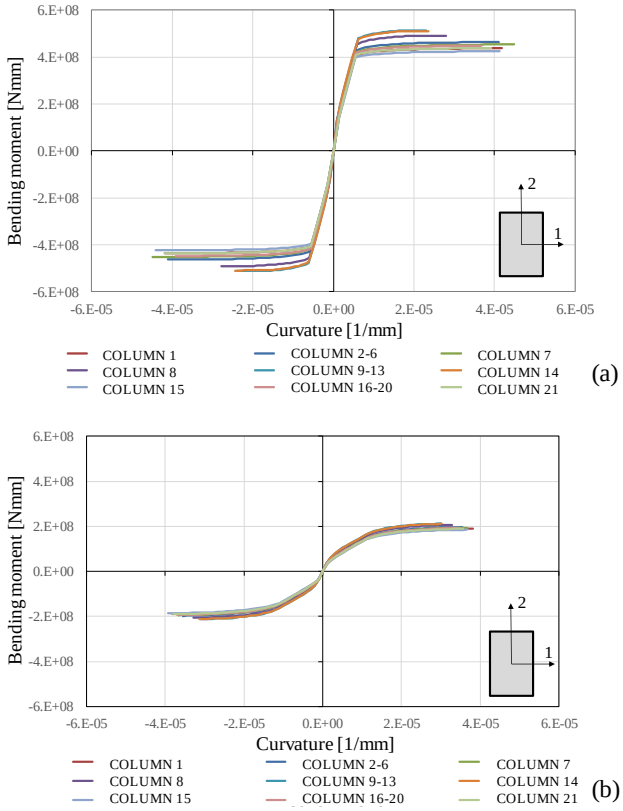

Figure 2. Moment – curvature relationships for columns around the local axis 1 (a) and 2 (b) at level LV0 – LV1.

A post-peak behaviour is assigned to moment-curvature curve by adding a descending branch. The final value of curvature is calculated by assuming 4.5 times the ultimate curvature, thus $4.5\chi_u$, as shown in Figure 3. Similarly, the moment – curvature relationships for the beams are assigned neglecting the axial force contribution.

In order to catch the post – peak response of the structure, the Arch Length convergence method is used in the last step of the analysis.

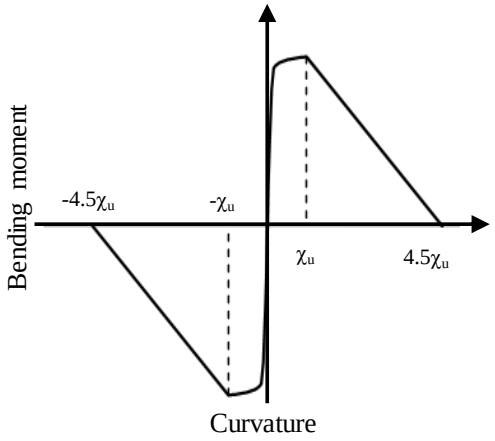

Figure 3. Softening assignment to the bending moment – curvature relationship.

Hence, the ductile mechanisms are modelled without interaction between bending moment, shear and axial behaviours. On the contrary, the shell modelling allows to properly take into account for axial force, shear force and bending moment interaction. In Figure 4 is reported the structure modelled using beam elements.

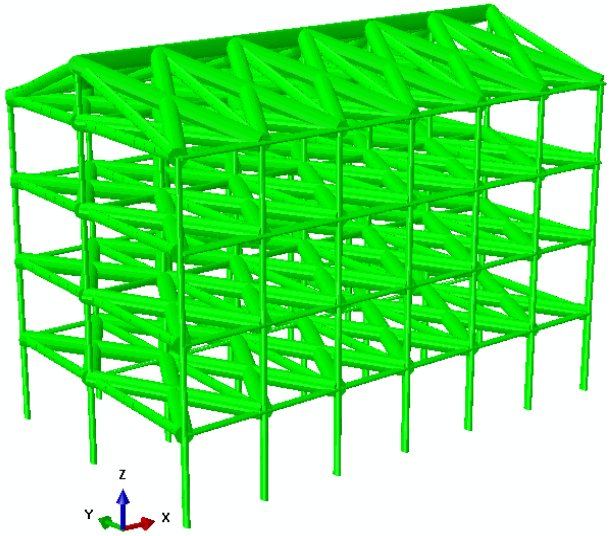

Figure 4. Beam element modelling.

2.4 *Multi-layered shell element modelling and PARC CL 2.0*

The nonlinear behaviour of beams and columns is modelled using multi-layered shell elements and the PARC_CL 2.0 crack model (Belletti et al. 2017a), implemented in Abaqus (Abaqus, 2018) as material user subroutine (see Figure 5). It is a fixed crack model where a smeared approach is assumed for the reinforcement hosted in the concrete element. The PARC_CL 2.0 crack model is suitable for a plane stress state, thus the thickness of the shell element can be subdivided into layers, each with concrete and/or steel properties.

The model has been initially developed to perform monotonic static analyses (Belletti et al., 2001), but its last version is able to account for hysteretic loops and plastic deformations for concrete and steel, considering the aggregate interlock (Belletti et al., 2017a, Belletti et al., 2017b). Particular applications concern the membrane effects of bridge deck slab (Belletti et al. 2015a, Belletti et al. 2015b) and continuous flat slabs (Belletti et al. 2016, Belletti et al., 2018a, Belletti et al., 2018b), and the lateral structural response of vertical wall systems (Belletti et al. 2013).

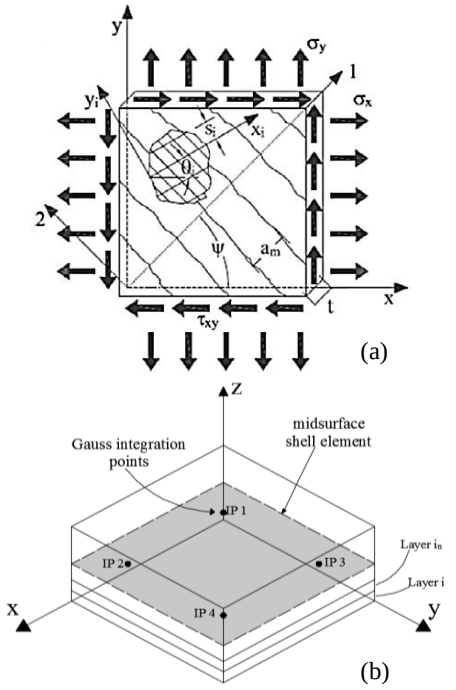

Figure 5. (a) PARC_CL 2.0 crack model; (b) Multi-layered shell model.

The constitutive laws adopted for concrete and steel are shown respectively in Figure 6 and Figure 7, based on the mean values reported in Table 1.

The diaphragm is modelled, as in the beam modelling, by means of truss T3D2 elements.

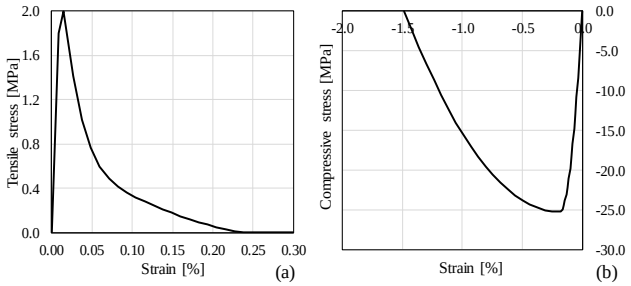

Figure 6. Concrete relationships for: (a) tensile stress – strain relation; (b) compressive stress – strain relation.

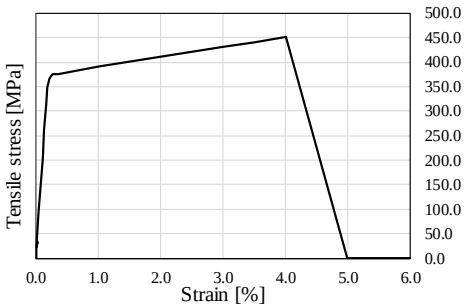

Figure 7. Stress strain relationship for longitudinal and transversal reinforcement.

The pushover analysis is carried out using a force control criteria with the traditional Newton-Raphson convergence algorithm.

The structure modelled using multi-layered shell elements is reported in Figure 8.

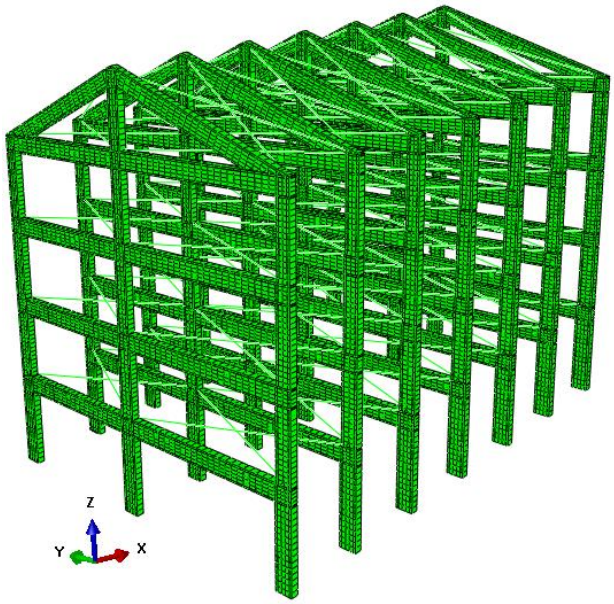

Figure 8. Shell element modelling.

3 DUCTILE AND BRITTLE FAILURE MECHANISMS

The chord rotations θ_y and θ_u for the evaluation of the ductile and brittle mechanisms can be calculated using the formulations provided by Eurocode 8 (Eurocode 8, 2005) and Italian NTC 2018 (NTC, 2018).

The yielding chord rotation θ_y for beams and columns can be calculated using Eq. 1:

$$\theta_y = \chi_y \frac{L_V}{3} + 0.0013\left(1+1.5\frac{h}{L_V}\right) + 0.13\chi_y \frac{d_b f_y}{\sqrt{f_c}} \quad (1)$$

where d_b is the average diameter of the longitudinal rebars, h is the height of the section, χ_y and χ_u are the yielding and ultimate curvatures, respectively, and L_V is the shear span.

The ultimate chord rotation θ_u for beams and columns can be calculated using Eq. 2:

$$\theta_u = \theta_y + (\chi_u - \chi_y) L_{pl} \left(1 - \frac{0.5 L_{pl}}{L_V}\right) \quad (2)$$

where L_{pl} is the plastic hinge length, calculated using Eq. 3:

$$L_{pl} = 0.1 L_V + 0.17 h + 0.24 \frac{d_b f_y}{\sqrt{f_c}} \quad (3)$$

The brittle failure mechanisms of beams and columns are evaluated by calculating the shear capacity of the seismic-resistant elements. The shear capacity V_R is calculated using the Biskinis formulation (Biskinis et al., 2004) provided in Eurocode 8 (Eurocode 8, 2005) and in the Italian NTC (NTC 2018), Eq. 4:

$$V_R = \frac{h-x}{2L_V} \min(N; 0.55 A_g f_c) + k \frac{A_w f_y d}{s} + \\ + k \left[0.16 \max(0.5; 100\rho_{tot}) \left(1 - 0.16 \min\left(5; \frac{L_V}{h}\right)\right) \sqrt{f_c} A_g \right] \quad (4)$$

where N is the axial force, x is the compressive depth and s is the spacing of stirrups. The formulations of θ_u and V_R are multiplied by a constant factor $1/\gamma_{el}$, where γ_{el} is taken as 1.15 for primary elements (assumed in this work) and 1 for secondary elements. The parameter k is given by Eq. 5:

$$k = 1 - 0.05 \min(5; \mu_\Delta^{pl}) \quad (5)$$

where the plastic contribution in ductility $\mu_{\Delta,pl}$ is calculated using Eq. 6:

$$\mu_\Delta^{pl} = \frac{\Delta - \Delta_y}{\Delta_y} = \frac{\theta - \theta_y}{\theta_y} \quad (6)$$

The limit value of the parameter k can range between the values of 1 and 0.75.

For the calculation of the brittle failures, a constant shear span length L_v equal to 0.5 times the floor to floor height is assumed.

In this study, also the beam-to-column joint behaviour is investigated, considering the case with and without the presence of stirrups.

For the case without stirrups, the tensile diagonal stress σ_{jt} is calculated by using Eq. 7:

$$\sigma_{jt} = \left| \frac{N}{2A_j} - \sqrt{\left(\frac{N}{2A_j}\right)^2 + \left(\frac{V_j}{A_j}\right)^2} \right| \le 0.3\sqrt{f_c} \quad (7)$$

where V_j is the shear demand on the joint. The compressive diagonal stress σ_{jc} is calculated using Eq. 8:

$$\sigma_{jc} = \frac{N}{2A_j} + \sqrt{\left(\frac{N}{2A_j}\right)^2 + \left(\frac{V_j}{A_j}\right)^2} \le 0.5 f_c \quad (8)$$

If the stirrups contribution N_{st} is considered, the tensile diagonal stress $\sigma_{jt,st}$ is calculated by using Eq. 9:

$$\sigma_{jt,st} = \left| \frac{N + N_{st}}{2A_j} - \sqrt{\left(\frac{N - N_{st}}{2A_j}\right)^2 + \left(\frac{V_j}{A_j}\right)^2} \right| \le 0.3\sqrt{f_c} \quad (9)$$

Generally, a beneficial contribution on the joint resistance should be expected considering the presence of stirrups, which provide a ductile behaviour to beam-to-column joints.

In the calculation of the shear and joint capacities, the mechanical parameters f_y and f_c are respectively f_{ym} and f_{cm} divided by the correspondent partial security factor γ_s and γ_c and by a confidence factor CF assumed equal to 1.

4 RESULTS AND DISCUSSION

The comparison between the beam element modelling and the multi-layered shell element approach is reported. In the paragraph 3.1 the comparison between the pushover analyses along the Y direction based on mass proportional acceleration is shown, while in the paragraphs 3.2 the different failure modes and damage levels are investigated for both modelling techniques.

4.1 Pushover analyses results

In Figure 9 are reported the base shear force vs displacement of the control point (corresponding to the central node at the level 4) curves for both beam and shell element models, with and without considering the geometrical nonlinearity.

Since a softening behaviour in the moment – curvature relationship is assigned to beam elements, and thanks to the Arch Length convergence method, the pushover curves obtained using the beam model is characterized by a post – peak softening branch.

For the shell element model, the pushover analyses are conducted using the Newton – Raphson convergence algorithm, due to problems detected using the Arch Length method coupled with the material user subroutine. For this reason, the pushover curves do not present a softening branch.

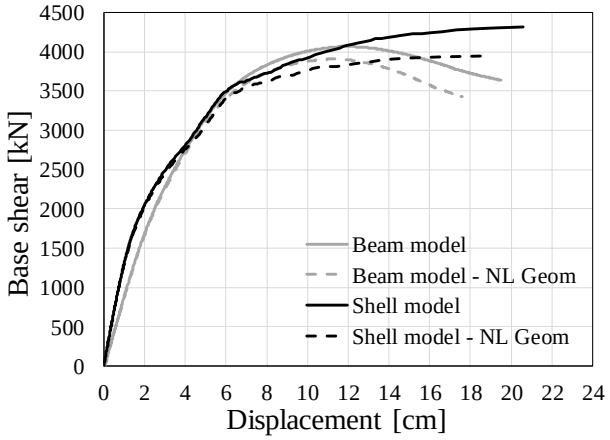

Figure 9. Base shear force versus control point displacement at level 4 for beam and shell modelling.

Shell element modelling takes into account for tensile strength and fracture energy of concrete not considered by beam modelling. As expected, more rigid behaviour can be observed for shell element model compared to the beam element model. The potentiality of identifying when and where cracking occurs, as well as the detecting of the strain, displacement and stress levels reached by concrete and steel during the NLFE analyses, is considered a powerful tool for the damage grade detection according to EMS98 (Grunthal, 1998). Indeed, shell element analysis, carried out using appropriate crack models, could be able to detect, on the basis of threshold values for specific engineering demand parameters, not only heavy damage levels but also slight or moderate damage levels for buildings.

In general, a good agreement between the curves obtained using beam and shell element modelling can be observed, also considering the geometrical nonlinearity.

4.2 Observed failure mechanisms

In this paragraph the comparison between ductile and brittle failure mechanisms are shown for beam and multi-layered shell element models.

4.2.1 Beam element modelling

The evaluation of ductile failures modes for beams and columns is carried out comparing the demand from NLFE analyses in terms of rotation with the capacity provided by Eq. (2). The chord rotation demand, for columns, is calculated by dividing the inter-storey drift by the floor to floor height.

The brittle failure modes for beams, columns and beam-to-column joints are calculated using a post-processing procedure, since beam modelling is not able to detect shear failure mode. For columns and beams the demand is obtained from NLFE analysis, while the capacity is obtained using Eq. (4).

The demand in beam-to-column joints is calculated from axial and shear forces in columns and bending moments in beams. The capacity in beam-to-column joints is calculated using Eqs. (7)-(9), neglecting or considering the presence of stirrups.

In Figure 10 is reported the sequence of events observed during the pushover analysis carried out using the beam element model.

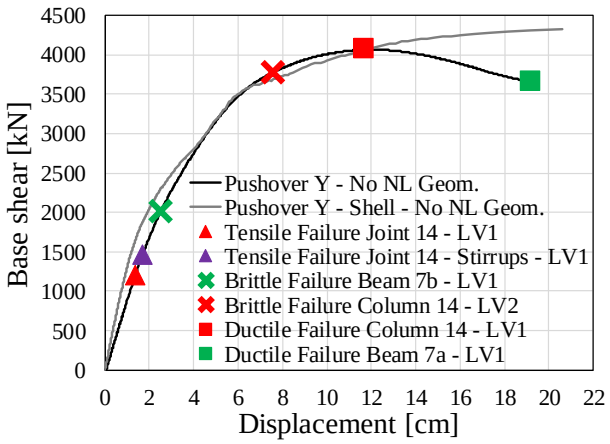

Figure 10. Base shear force versus control point displacement at level 4 for beam and shell modelling: sequence of events.

The sequence of events corresponds to:

- The beam-to-column joint 14 (Figure 1) failure at the first level due to cracking and neglecting the presence of stirrups, Eq. (7). In engineering practice, the achievement of this failure mode would lead to a repairing action characterised by strengthening of joints to improve the structural performances. The compressive strength is not achieved.
- The beam-to-column joint 14 failure at the first level due to cracking considering the presence of stirrups, Eq. (9). The compressive strength is not achieved.
- The shear failure of the shorter beam 7b (Figure 1) at the first level;
- The shear failure of the column 14 (Figure 1) at the second level;
- The peak of the pushover curve corresponds to the capacity of the structure, where the ductile failure of the column 14 at the first level is achieved;
- The ductile failure of the beam 7a (Figure 1) at the first level.

The deformed shapes of the beam and shell element models are shown in correspondence of the peak load of the pushover analyses, recorded at a displacement of 12 cm, see Figure 11. The red

dot indicates the control point of the fourth level where the displacement is recorded. It is interesting to observe that the structure exhibits higher displacements in correspondence of the right side of the building, due to the mass distribution. Therefore, more several actions on frames placed at the right side of the structure (like the columns 7, 14, 21 and the beams 7a and 7b, see Figure 1) should be expected.

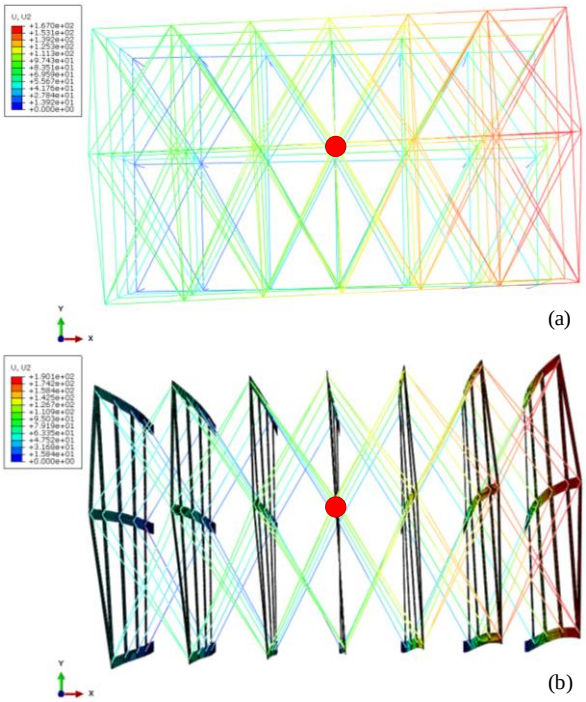

Figure 11. Deformed shape (x10) at the peak load for: (a) beam element model and (b) shell element model.

4.2.2 Shell element modelling

In this paragraph, the heavy damage grade obtained using beam modelling is compared with the damage grade obtained using shell elements. In particular, the brittle failure modes in beams, columns and beam-to-column joints, obtained using beam modelling are critically commented on the basis of shell element modelling results.

Firstly, the beam-to-column joints failure modes, achieved in joint 14, are remarked using post-processing of beam modelling results and verifications according to Eqs. (7) – (9). In Figure 12, in correspondence of the beam-to-column joint 14 at the first level, the values of the normalized tensile stresses of concrete, the compressive diagonal concrete stresses and stresses in stirrups are plotted, versus the angular deformation, γ, of the beam-to-column joint. From Figure 12, can be pointed out that the tensile strength in concrete is reached (i.e. the joint is cracked), while the concrete strength in compression is not achieved, as obtained from beam element model coupled with analytical formulations. The ductility of the beam-to-column joint is given by stirrups that reach the yielding and allow the transmission of internal forces in joints. Therefore, the main difference between analytical and NLFE analysis results can be explained as follows: for analytical calculation the capacity is detected at cracking, while, using shell element modelling, the joint capacity can be evaluated also after cracking, considering the contribution of all the phenomena like residual tensile stresses due to fracture energy of concrete, aggregate interlocking and non-linear stress-strain relationships for stirrups and longitudinal reinforcement.

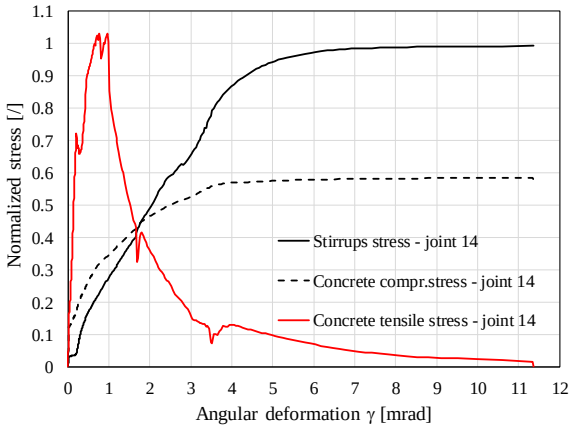

Figure 12. Shell modelling: normalized stresses vs angular deformation γ of the beam-to-column joint 14 at level 1.

In Figure 13 the contours of the minimum principal stress and the tensile concrete strain are reported for the levels 1 and 2. The model is able to detect the compressive stress flow through beams and columns (Figure 13a) and the zones where the cracking of concrete is reached (Figure 13b).

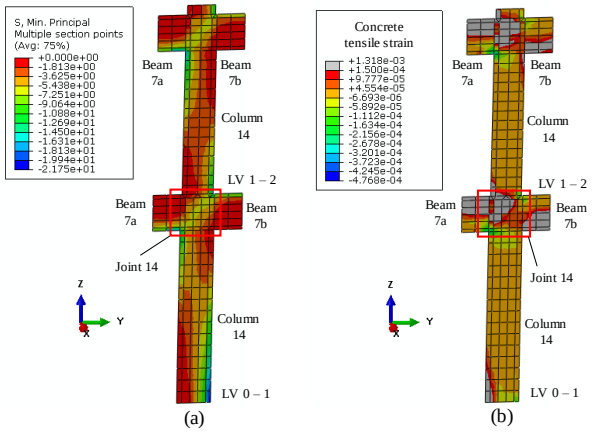

Figure 13. Joint 14: (a) minimum principal stress flow contour; (b) tensile concrete strain contour, at a displacement of 1.5 cm.

In Figure 14 the normalized rebar stresses and the angular deformation, γ, in beam 7a and column 14 (in correspondence of the joint 14 at the first level) are reported as function of the control point displacement. The first ductile failure is detected in correspondence of the column 14, followed by the ductile failure of the beam 7a. It is interesting to observe an almost constant value of the angular deformation γ detected in correspondence of the beam failure, indicating that the joint shows a rigid motion along the column height after the beam failure.

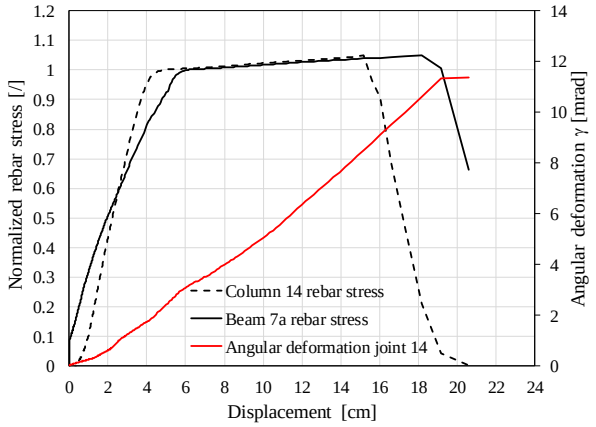

Figure 14. Shell modelling: normalized rebar stresses for beam 7a and column 14 and angular deformation γ of the beam-to-column joint 14 vs displacement at level 1.

In Figure 15 the contours of the rebars and stirrups strains are shown for beam-to-column joint 14 when the ductile failure of the beam 7a is achieved. The longitudinal rebars are widely yielded (in grey in Figure 15a) and the steel rupture (ε_{rup} = 4 %) is observed before at the base of the column and later in correspondence of the beams. The transversal rebars show widely yielded zones (in grey in Figure 15b) but the steel rupture strain (ε_{rup} = 4 %) is not achieved.

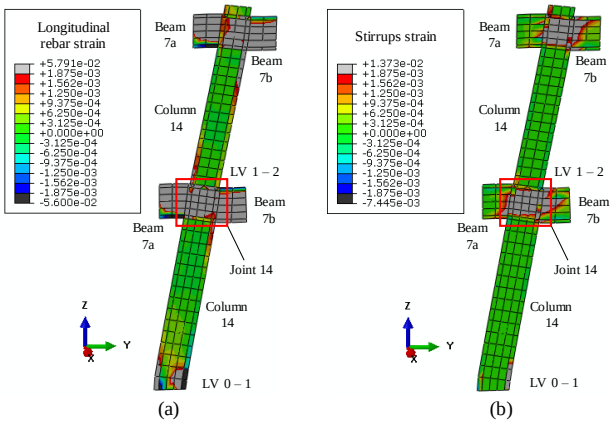

Figure 15. Rebar contour: (a) longitudinal rebar strain contour; (b) transversal rebar strain contour, for a displacement of 20 cm.

The mentioned observations show how the analysed beam-to-column joint is able to exhibit a considerable ductility.

It is important to observe that the shell element model does not detect shear failure of beams and columns, in contrast with the beam element model. This is caused by the fact that for the latter, the mechanical strengths of steel f_{ym} and concrete f_{cm} are not divided by the respectively partial security factors. Indeed, for the brittle failure formulations, if the mechanical properties are assumed as not affected by the partial security factors, also the beam element model does not detect shear failures.

Finally, it is clear how the shell element model, conversely to the beam element model, is able to catch different damage grades during the pushover analysis, due to the detailed nonlinear relationships of concrete and steel, for example cracking of concrete, aggregate interlock, yielding and rupture of longitudinal and/or transversal reinforcement.

5 CONCLUSIONS

In this study, the finite element modelling of the institute “A. De Gasperi – R. Battaglia” located in Norcia is shown by using beam and multi-layered shell elements. The main conclusions of this study are:

- Referring to the damage grades described in the EMC98 document, it can be observed how the multi-layered shell element model is suitable to capture the different acceleration stages which characterize the structural response of the building (concrete cracking, steel yielding etc.). This is due to the capacity of the modelling technique to capture the detailed interaction between steel and concrete.
- Both beam and multi-layered shell element models are able to catch the critical members located at the right side of the building;
- The beam element model detects the failure of the beam-to-column joint 14 in correspondence of low accelerations, instead, the shear failure of the column 14 is individuated for higher accelerations, which anticipates the ductile failure of the member;
- The multi-layered shell element model is able to capture the cracking of the beam-to-column joint 14. Furthermore, due to the presence of stirrups and the detailed interaction between concrete and reinforcement, the joint continues to

transfer the internal forces between beams and columns;

- The multi-layered shell element model does not show brittle failures, thus, the peak of the structural response corresponds to the achievement of the ductile failure at the base of the column 14;
- This case study is helpful to highlight how simplified models, such as beam element modelling coupled with conservative formulations provided by Codes, could lead to damage mechanisms and damage grades which are different from the realistic behaviour of the structure. For this reason, the interventions aimed at improving the seismic performances of buildings could be sometimes useless.
- A methodical comparison between the results obtained by different modelling techniques could be useful in order to optimize the intervention strategies.

6 ACKNOWLEDGEMENTS

This paper is supported by the Italian research project RELUIS 2019-2021.

7 REFERENCES

Abaqus 2018. User's and Theory Manuals 2018.

Belletti, B., Cerioni, R., Iori, I. 2001. Physical approach for reinforced-concrete (PARC) membrane elements. *ASCE J Struct Eng*, 2001, 127(12), pp.1412–26.

Belletti, B., Damoni, C., Gasperi, A. 2013. Modeling approaches suitable for pushover analyses of RC structural wall buildings. *Eng. Struct.* 2013b;57(12), pp.327–38

Belletti, B., Walraven, J.C., Trapani, F. 2015a. Evaluation of compressive membrane action effects on punching shear resistance of reinforced concrete slabs. *Engineering Structures*, 95(7): 25-39.

Belletti, B., Pimentel M., Scolari M., Walraven, J.C. 2015b. Safety assessment of punching shear failure according to level of approximation approach. *Structural Concrete, 16(3): 366-380*.

Belletti B., Cantone R., Manelli L., Muttoni A. 2016. Compressive membrane action effects on punching strength of flat RC slabs. *8th International Conference on Concrete under Severe Conditions -- Environment and Loading*, Lecco, Italy, 12-14 September

Belletti, B., Scolari, M., Vecchi, F. 2017a. PARC_CL 2.0 crack model for NLFEA of reinforced concrete structures under cyclic loadings. *Computers and Structures*, 191, 165–79.

Belletti, B., Scolari, M., Stocchi, A., Vecchi, F. 2017b. Validation of the PARC_CL 2.0 crack model for the assessment of the nonlinear behaviour of RC structures subjected to seismic action: SMART 2013 shaking table test simulation. *Eng. Struct.* 150, pp.759-73.

Belletti, B., Muttoni, A., Ravasini, S., Vecchi, F. 2018a. Parametric analysis on punching shear resistance of reinforced-concrete continuous slabs. *Mag. of Concrete Research*, https://doi.org/10.1680/jmacr.18.00123.

Belletti, B., Muttoni, A., Ravasini, S., Vecchi, F. 2018b. Dependency of punching shear resistance and membrane action on boundary conditions of reinforced concrete continuous slabs. *The Sixth International Symposium on Life-Cycle Civil Engineering, IALCCE 2018, Ghent University, Belgium*.

Dionysis, E., Biskinis, George, K. Roupakias, Michael N. Fardis, 2004. Degradation of Shear Strength of Reinforced Concrete Members with Inelastic Cyclic Displacements. *ACI Structural Journal*, V. 101, No. 6, November-December 2004.

Grunthal, G. (1998), "European Macroseismic Scale 1998", *Cahiers du Centre Europ. de Géodyn. et de Séismlogie* vol 15: 1-99.

Lima, C., Angiolilli, M., Barbagallo, F., Belletti, B., Bergami, A. V., Camata, G., Cantagallo, C., Di Domenico, M., Fiorentino, G., Ghersi, A., Gregori, A., Lavorato, D., Luciano, R., Marino, E.M., Martinelli, E., Nuti, C., Ricci, P., Rosati, L., Ruggieri, S., Sessa, S., Spacone, E., Terrenzi, M., Uva, G., Vecchi, F., Verderame, G.M 2018. Nonlinear modeling techniques for existing buildings in reinforced concrete: the case study of De Gasperi-Battaglia Institute of Norcia. *Proceedings of Italian Concrete Days 2018.*

NTC 2018. Norme Tecniche per le Costruzioni. D.M. 17 gennaio 2018.

UNI EN 1998-1-8:2005. Eurocode 8: design of structures for earthquake resistance.